



ARL-TR-7346 • JUL 2015



Scattering from the Finite-Length, Dielectric Circular Cylinder: Part I—Derivation of an Analytical Solution

by DaHan Liao

Approved for public release; distribution unlimited.

NOTICES

Disclaimers

The findings in this report are not to be construed as an official Department of the Army position unless so designated by other authorized documents.

Citation of manufacturer's or trade names does not constitute an official endorsement or approval of the use thereof.

Destroy this report when it is no longer needed. Do not return it to the originator.



Scattering from the Finite-Length, Dielectric Circular Cylinder: Part I—Derivation of an Analytical Solution

by DaHan Liao

Sensors and Electron Devices Directorate, ARL

REPORT DOCUMENTATION PAGE				Form Approved OMB No. 0704-0188	
<p>Public reporting burden for this collection of information is estimated to average 1 hour per response, including the time for reviewing instructions, searching existing data sources, gathering and maintaining the data needed, and completing and reviewing the collection information. Send comments regarding this burden estimate or any other aspect of this collection of information, including suggestions for reducing the burden, to Department of Defense, Washington Headquarters Services, Directorate for Information Operations and Reports (0704-0188), 1215 Jefferson Davis Highway, Suite 1204, Arlington, VA 22202-4302. Respondents should be aware that notwithstanding any other provision of law, no person shall be subject to any penalty for failing to comply with a collection of information if it does not display a currently valid OMB control number.</p> <p>PLEASE DO NOT RETURN YOUR FORM TO THE ABOVE ADDRESS.</p>					
1. REPORT DATE (DD-MM-YYYY) July 2015		2. REPORT TYPE Final		3. DATES COVERED (From - To) January 2015–March 2015	
4. TITLE AND SUBTITLE Scattering from the Finite-Length, Dielectric Circular Cylinder: Part I— Derivation of an Analytical Solution				5a. CONTRACT NUMBER	
				5b. GRANT NUMBER	
				5c. PROGRAM ELEMENT NUMBER	
6. AUTHOR(S) DaHan Liao				5d. PROJECT NUMBER	
				5e. TASK NUMBER	
				5f. WORK UNIT NUMBER	
7. PERFORMING ORGANIZATION NAME(S) AND ADDRESS(ES) US Army Research Laboratory ATTN: RDRL-SER-U 2800 Power Mill Road Adelphi, MD 20783-1197				8. PERFORMING ORGANIZATION REPORT NUMBER ARL-TR-7346	
9. SPONSORING/MONITORING AGENCY NAME(S) AND ADDRESS(ES)				10. SPONSOR/MONITOR'S ACRONYM(S)	
				11. SPONSOR/MONITOR'S REPORT NUMBER(S)	
12. DISTRIBUTION/AVAILABILITY STATEMENT Approved for public release; distribution unlimited.					
13. SUPPLEMENTARY NOTES					
14. ABSTRACT Given that an understanding of the scattering effects of the cylinder is important in characterizing the electromagnetic responses of tree structures, in this work a closed-form, approximate formulation is derived for the scattering matrix of the finite-length, dielectric circular cylinder. The solution is obtained by applying the modal (or eigenfunction) expansion method in conjunction with the volumetric equivalence principle, and supposes that the internal fields of the finite-length cylinder are the same as those of the infinite-length case. The theory is first developed for the scatterer located in free space. Subsequently, the problem of the scatterer located above a finite-conducting ground is considered by employing a multiray technique in which the total scattering response is calculated by coherently summing the direct response and the single and double ground bounce contributions. An arbitrarily oriented cylinder is treated by augmenting the solution with appropriate coordinate transformation matrices. This study is intended to facilitate the development of a discrete scatterer approach for characterizing the scattering from tree canopies.					
15. SUBJECT TERMS Foliage-penetration radar, tree scattering					
16. SECURITY CLASSIFICATION OF:			17. LIMITATION OF ABSTRACT UU	18. NUMBER OF PAGES 20	19a. NAME OF RESPONSIBLE PERSON DaHan Liao
a. REPORT Unclassified	b. ABSTRACT Unclassified	c. THIS PAGE Unclassified			19b. TELEPHONE NUMBER (Include area code) (301) 394-1741

Contents

List of Figures	iv
1. Introduction	1
2. Semi-Exact Solution in Free Space	2
3. Multiray Solution in the Presence of a Half Space	8
4. Numerical Results	9
5. Conclusions	11
6. References	12
Distribution List	14

List of Figures

- Fig. 1 Backscattering cross section (as function of frequency) of a tilted, finite-length, dielectric circular cylinder located in free space and above a half space: $\nu\nu$ response. Parameters: $a = 15$ cm; $L = 7.5$ m; $\theta_i = 40^\circ$; and $\phi_i = 200^\circ$ 10
- Fig. 2 Backscattering cross section (as function of frequency) of a tilted, finite-length, dielectric circular cylinder located in free space and above a half space: hh response. Parameters are the same as those in Fig. 1. 10
- Fig. 3 Backscattering cross section (as function of frequency) of a tilted, finite-length, dielectric circular cylinder located in free space and above a half space: $h\nu$ response. Parameters are the same as those in Fig. 1..... 11

1. Introduction

Various theoretical scattering models have been developed over the years for characterizing the electromagnetic responses of trees within the context of microwave remote sensing and foliage-penetrating radar applications.^{1–15} These research efforts can be loosely categorized into 2 main classes: The first class is derived from radiative transfer theory, which assumes the tree canopy to be a uniform layer containing a random distribution of scatterers and relies on the use of statistical averages for the calculation of extinction, source, and phase matrices (or coefficients); the second class is based on the so-called discrete scatterer approach, which is a more deterministic method that seeks to directly account for individual scattering mechanisms. (Note that a vegetation canopy can also be treated as a continuous medium with a fluctuating permittivity function; this approach, however, is most appropriate and tractable for weakly scattering media in which the fluctuating function is small relative to its mean value.⁵) While traditional radiative transfer theory has been applied successfully to a number of remote sensing scenarios involving complex forest canopy structures,¹⁶ this method does not account for the coherent scattering effects occurring within the tree structure and therefore cannot be used to compute the phase response of a scene. On the contrary, the discrete scatterer approach—which first decomposes a tree structure (trunk, branch complex, and leaves/needles) into simple-shaped scatterers such as finite-length dielectric cylinders and dielectric disks and then calculates the collective return by summing the scattered fields from each scatterer—is a coherent technique that can be employed to deduce the generalized polarimetric response. The development of the discrete scatterer approach, then, is dependent upon a thorough understanding of the scattering effects of dielectric cylinders and disks—preferably through the derivation of closed-form expressions for their scattering matrices. The subject of interest in this work is the scattering from a finite-length, dielectric circular cylinder, which is the elementary component used to model the trunk and branching structure of a tree. (The leaves/needles of a tree are commonly approximated as disks. At the lower frequency bands, the effects of the leaves/needles are often assumed to be negligible; thus, a study of the scattering from disks is not included in the current work.)

The organization of the work is as follows. In Section 2 a complete derivation of the scattering matrix of the finite-length, dielectric circular cylinder is presented. A closed-form, approximate solution is obtained by applying the modal (or eigen-function) expansion method in conjunction with the volumetric equivalence

principle; the formulation exploits the supposition that the internal fields of the finite-length cylinder are the same as those of the infinite-length case. The theory is first developed for a cylinder in free space. Subsequently, the problem of the cylinder located above a finite-conducting ground is considered in Section 3, in which a multiray technique is employed to deal with the effects of the half space; essentially, this approach calculates the total scattering response by coherently summing the first-order direct response and the single and double ground bounce contributions. An arbitrarily oriented cylinder is treated by augmenting the solution with appropriate coordinate transformation matrices. In Section 4, simulation results are presented to demonstrate the utility of the analytical solution. Finally, in Section 5, a summary of the overall work is given.

2. Semi-Exact Solution in Free Space

In the current problem, the incident and scattered wave directions (\hat{k}_i, \hat{k}_s) and their associated polarization vectors (\hat{h}, \hat{v}) are defined by

$$\hat{k}_i = \sin \theta_i \cos \phi_i \hat{x} + \sin \theta_i \sin \phi_i \hat{y} - \cos \theta_i \hat{z}; \quad (1)$$

$$\hat{k}_s = \sin \theta_s \cos \phi_s \hat{x} + \sin \theta_s \sin \phi_s \hat{y} + \cos \theta_s \hat{z}; \quad (2)$$

$$\hat{h}_{i,s} = \frac{\hat{z} \times \hat{k}_{i,s}}{|\hat{z} \times \hat{k}_{i,s}|}; \quad (3)$$

$$\hat{v}_{i,s} = \hat{h}_{i,s} \times \hat{k}_{i,s}; \quad (4)$$

in which the subscripts i and s identify quantities related to the incident and scattered waves, respectively; θ_i is the incidence angle in elevation (measured from $-\hat{z}$); θ_s is the scattering angle in elevation (measured from $+\hat{z}$); and $\phi_{i,s}$ is the incidence/scattering angle in azimuth (measured from $+\hat{x}$). Without the loss of generality, a vertically polarized (TM_z) plane wave is taken as the source of excitation; that is, with time convention of $e^{j\omega t}$ and designating the wave number in free space as k_o , the incident electric field is simply $\vec{E}^i(\vec{r}) = E_o \hat{v}_i e^{-jk_o \hat{k}_i \cdot \vec{r}}$. This wave is impinging on a dielectric circular cylinder with radius a and relative dielectric constant ϵ_r . Here, for the initial discussions, the cylinder is centered at the origin, with its axis aligned with the z -axis. The first step is to derive the fields inside an infinite-length cylinder—which has an exact modal solution; subsequently, the scattering response of the finite-length case is deduced by approximating the cylinder's internal fields with those of the infinite-length case.

It can be shown that the z -component of the electric field of the incident wave can be expanded as

$$E_z^i(\rho, \phi, z) = \tilde{E}_o \sum_{n=-\infty}^{+\infty} j^{-n} J_n(k_{\rho,i} \rho) e^{jn(\phi-\phi_i)}, \quad (5)$$

with $\tilde{E}_o = -E_o \sin \theta_i e^{jk_{z,i}z}$, $k_{z,i} = k_o \cos \theta_i$, and $k_{\rho,i} = k_o \sin \theta_i$. Note that $H_z^i = 0$ for a TM_z wave. It is theorized that the z -components of the scattered and internal electric and magnetic fields of the infinite-length cylinder can be written in the following forms:

$$E_z^s(\rho, \phi, z) = \tilde{E}_o \sum_{n=-\infty}^{+\infty} A_n H_n^{(2)}(k_{\rho,i} \rho) e^{jn(\phi-\phi_i)}; \quad (6)$$

$$E_z^d(\rho, \phi, z) = \tilde{E}_o \sum_{n=-\infty}^{+\infty} B_n J_n(k_{\rho,r} \rho) e^{jn(\phi-\phi_i)}; \quad (7)$$

$$H_z^s(\rho, \phi, z) = \tilde{E}_o \sum_{n=-\infty}^{+\infty} C_n H_n^{(2)}(k_{\rho,i} \rho) e^{jn(\phi-\phi_i)}; \quad (8)$$

$$H_z^d(\rho, \phi, z) = \tilde{E}_o \sum_{n=-\infty}^{+\infty} D_n J_n(k_{\rho,r} \rho) e^{jn(\phi-\phi_i)} \quad (9)$$

where $k_{\rho,r} = k_o \sqrt{\epsilon_r - \cos^2 \theta_i}$; and A_n , B_n , C_n , and D_n are unknowns to be determined.

Noting that

$$E_\phi \left(1 - \frac{k_{z,i}^2}{\omega^2 \mu \epsilon} \right) = \frac{-k_{z,i}}{j \omega^2 \mu \epsilon} \cdot \frac{1}{\rho} \cdot \frac{\partial E_z}{\partial \phi} - \frac{1}{j \omega \epsilon} \cdot \frac{\partial H_z}{\partial \rho}; \quad (10)$$

$$H_\phi \left(1 - \frac{k_{z,i}^2}{\omega^2 \mu \epsilon} \right) = \frac{-k_{z,i}}{j \omega^2 \mu \epsilon} \cdot \frac{1}{\rho} \cdot \frac{\partial H_z}{\partial \phi} + \frac{1}{j \omega \mu} \cdot \frac{\partial E_z}{\partial \rho}, \quad (11)$$

the ϕ -components of the same set of electric and magnetic fields can be formulated as follows:

$$E_\phi^i(\rho, \phi, z) = -\tilde{E}_o \cdot \frac{\cos \theta_i}{k_o \rho \sin^2 \theta_i} \sum_{n=-\infty}^{+\infty} j^{-n} n J_n(k_{\rho,i} \rho) e^{jn(\phi-\phi_i)}; \quad (12)$$

$$E_{\phi}^s(\rho, \phi, z) = \tilde{E}_o \sum_{n=-\infty}^{+\infty} \left[\frac{-\cos \theta_i}{k_o \rho \sin^2 \theta_i} n A_n H_n^{(2)}(k_{\rho,i} \rho) - \frac{k_o}{j \omega \varepsilon_o \sin \theta_i} C_n H_n^{(2)'}(k_{\rho,i} \rho) \right] e^{jn(\phi - \phi_i)}; \quad (13)$$

$$E_{\phi}^d(\rho, \phi, z) = \tilde{E}_o \sum_{n=-\infty}^{+\infty} \left[\frac{-\cos \theta_i}{k_o \rho (\varepsilon_r - \cos^2 \theta_i)} n B_n J_n(k_{\rho,r} \rho) - \frac{k_o}{j \omega \varepsilon_o \sqrt{\varepsilon_r - \cos^2 \theta_i}} D_n J_n'(k_{\rho,r} \rho) \right] e^{jn(\phi - \phi_i)}; \quad (14)$$

$$H_{\phi}^i(\rho, \phi, z) = \tilde{E}_o \cdot \frac{k_o}{j \omega \mu_o \sin \theta_i} \sum_{n=-\infty}^{+\infty} j^{-n} J_n'(k_{\rho,i} \rho) e^{jn(\phi - \phi_i)}; \quad (15)$$

$$H_{\phi}^s(\rho, \phi, z) = \tilde{E}_o \sum_{n=-\infty}^{+\infty} \left[\frac{-\cos \theta_i}{k_o \rho \sin^2 \theta_i} n C_n H_n^{(2)}(k_{\rho,i} \rho) + \frac{k_o}{j \omega u_o \sin \theta_i} A_n H_n^{(2)'}(k_{\rho,i} \rho) \right] e^{jn(\phi - \phi_i)}; \quad (16)$$

$$H_{\phi}^d(\rho, \phi, z) = \tilde{E}_o \sum_{n=-\infty}^{+\infty} \left[\frac{-\cos \theta_i}{k_o \rho (\varepsilon_r - \cos^2 \theta_i)} n D_n J_n(k_{\rho,r} \rho) + \frac{\varepsilon_r k_o}{j \omega u_o \sqrt{\varepsilon_r - \cos^2 \theta_i}} B_n J_n'(k_{\rho,r} \rho) \right] e^{jn(\phi - \phi_i)}. \quad (17)$$

The unknowns A_n , B_n , C_n , and D_n can be found by matching the tangential electric and magnetic-field components at the cylinder's surface. It can be shown that

$$A_n = \frac{j^{-n}}{H_n^{(2)}(k_{\rho,i} a)} \cdot \left[\frac{-j}{R_n} M_n - J_n(k_{\rho,i} a) \right]; \quad (18)$$

$$B_n = \frac{-j^{-n+1} M_n}{J_n(k_{\rho,r} a) R_n}; \quad (19)$$

$$C_n = D_n \frac{J_n(k_{\rho,r} a)}{H_n^{(2)}(k_{\rho,i} a)}; \quad (20)$$

$$D_n = \frac{-j^{-n} k_o n W \cos \theta_i}{\omega u_o J_n(k_{\rho,r} a) R_n}; \quad (21)$$

where

$$R_n = \frac{\pi (k_{\rho,i} a)^2 H_n^{(2)}(k_{\rho,i} a)}{2} \cdot [M_n \cdot N_n - W^2 n^2 \cos^2 \theta_i]; \quad (22)$$

$$M_n = \tilde{H}_n(k_{\rho,i} a) - \tilde{J}_n(k_{\rho,r} a); \quad (23)$$

$$N_n = \tilde{H}_n(k_{\rho,i} a) - \varepsilon_r \tilde{J}_n(k_{\rho,r} a); \quad (24)$$

$$\tilde{H}_n(k_{\rho,i} a) = \frac{H_n^{(2)'}(k_{\rho,i} a)}{k_{\rho,i} a H_n^{(2)}(k_{\rho,i} a)}; \quad (25)$$

$$\tilde{J}_n(k_{\rho,r} a) = \frac{J_n'(k_{\rho,r} a)}{k_{\rho,r} a J_n(k_{\rho,r} a)}; \quad (26)$$

$$W = \frac{1}{(k_{\rho,i} a)^2} - \frac{1}{(k_{\rho,r} a)^2}. \quad (27)$$

Consequently, the ρ -component of the electric field inside the cylinder can be expressed as

$$E_\rho^d(\rho, \varphi, z) = \tilde{E}_o \sum_{n=-\infty}^{+\infty} \left[\left(\frac{n D_n}{\omega \varepsilon_r \varepsilon_o \rho} \right) \cdot \left(1 - \frac{\cos^2 \theta_i}{\varepsilon_r - \cos^2 \theta_i} \right) J_n(k_{\rho,r} \rho) + \frac{j B_n \cos \theta_i}{\sqrt{\varepsilon_r - \cos^2 \theta_i}} J_n'(k_{\rho,r} \rho) \right] e^{jn(\phi - \phi_i)}. \quad (28)$$

The fields inside an infinite-length cylinder $\vec{E}^d(\rho, \phi, z)$ are then completely characterized by Eqs. 7, 14, and 28.

In view of the volumetric equivalence principle, an approximate solution for the scattering response $\vec{E}^s(r, \theta_s, \phi_s)$ of a cylinder with length L can be calculated using the internal fields of the infinite-length problem treated above; that is, in the far field,

$$\vec{E}^s(r, \theta_s, \phi_s) = \frac{e^{-jk_o r}}{4\pi r} \int_{-L/2}^{+L/2} \int_0^a \int_0^{2\pi} k_o^2 (\varepsilon_r - 1) (\hat{h}_s \hat{h}_s + \hat{v}_s \hat{v}_s) \cdot \vec{E}^d(\rho', \phi', z') e^{jk_o \hat{k}_s (\rho' \hat{\rho}' + z' \hat{z}')} \rho' d\phi' d\rho' dz'. \quad (29)$$

After substituting Eqs. 7, 14, and 28 into 29, the integration over the cylinder's volume can be facilitated by noting the following relations:

$$\int_{-L/2}^{+L/2} e^{jk_o z' (\cos \theta_i + \cos \theta_s)} dz' = L \text{sinc} \left(\frac{k_o L (\cos \theta_i + \cos \theta_s)}{2} \right); \quad (30)$$

$$\int_0^{2\pi} \cos \phi' e^{jk_{\rho,s} \rho' \cos(\phi' - \phi_s) + jn(\phi' - \phi_i)} d\phi' = -2\pi j^n \left[j \cos \phi_s J_n'(k_{\rho,s} \rho') + \frac{n \sin \phi_s}{k_{\rho,s} \rho'} J_n(k_{\rho,s} \rho') \right] e^{jn(\phi_s - \phi_i)} = \bar{C}_n; \quad (31)$$

$$\int_0^{2\pi} \sin \phi' e^{jk_{\rho,s} \rho' \cos(\phi' - \phi_s) + jn(\phi' - \phi_i)} d\phi' = -2\pi j^n \left[j \sin \phi_s J_n'(k_{\rho,s} \rho') - \frac{n \cos \phi_s}{k_{\rho,s} \rho'} J_n(k_{\rho,s} \rho') \right] e^{jn(\phi_s - \phi_i)} = \bar{S}_n; \quad (32)$$

$$\begin{aligned} & \frac{1}{4\pi} \int_0^a j^{-n} \left[\left(ja' J_n'(k_{\rho,r} \rho') + \frac{nb'}{k_{\rho,r} \rho'} J_n(k_{\rho,r} \rho') \right) \bar{S}_n - \left(\frac{na'}{k_{\rho,r} \rho'} J_n(k_{\rho,r} \rho') - jb' J_n'(k_{\rho,r} \rho') \right) \bar{C}_n \right] \rho' d\rho' \\ &= \frac{1}{4} \left[(b' - ja') I_{n+1} e^{j\phi_s} + (b' + ja') I_{n-1} e^{-j\phi_s} \right] e^{jn(\phi_s - \phi_i)}; \end{aligned} \quad (33)$$

$$\begin{aligned} & \frac{1}{4\pi} \int_0^a j^{-n} \left[\left(ja' J_n'(k_{\rho,r} \rho') + \frac{nb'}{k_{\rho,r} \rho'} J_n(k_{\rho,r} \rho') \right) \bar{C}_n + \left(\frac{na'}{k_{\rho,r} \rho'} J_n(k_{\rho,r} \rho') - jb' J_n'(k_{\rho,r} \rho') \right) \bar{S}_n \right] \rho' d\rho' \\ &= \frac{j}{4} \left[(b' - ja') I_{n+1} e^{j\phi_s} - (b' + ja') I_{n-1} e^{-j\phi_s} \right] e^{jn(\phi_s - \phi_i)}; \end{aligned} \quad (34)$$

$$\int_0^a J_n(k_{\rho,r} \rho') J_n(k_{\rho,s} \rho') \rho' d\rho' = I_n; \quad (35)$$

where

$$I_n = \frac{a^2}{(k_{\rho,r}a)^2 - (k_{\rho,s}a)^2} (k_{\rho,r}a J_n(k_{\rho,s}a) J_{n+1}(k_{\rho,r}a) - k_{\rho,s}a J_n(k_{\rho,r}a) J_{n+1}(k_{\rho,s}a)); \quad (36)$$

$$k_{\rho,s} = k_o \sin \theta_s. \quad (37)$$

After much algebraic manipulation, the scattering matrix elements corresponding to a vertically polarized excitation wave are shown to be given by

$$S_{pv}^l(\hat{k}_s, \hat{k}_i) = \hat{p}_s \cdot \frac{k_o^2 (\epsilon_r - 1) L}{2} \text{sinc} \left(\frac{k_o L (\cos \theta_i + \cos \theta_s)}{2} \right) \sum_{n=-\infty}^{+\infty} [\vec{K}_{1,n} + \vec{K}_{2,n} + \vec{K}_{3,n}] e^{jn(\phi_s - \phi_i)}, \quad (38)$$

where $p = v, h$ and

$$\vec{K}_{1,n} = \frac{jk_o I_{n+1} e^{j\phi_s}}{2k_{\rho,r}} (\beta_n - j\alpha_n) (\hat{x} - j\hat{y}); \quad (39)$$

$$\vec{K}_{2,n} = -\frac{jk_o I_{n-1} e^{-j\phi_s}}{2k_{\rho,r}} (\beta_n + j\alpha_n) (\hat{x} + j\hat{y}); \quad (40)$$

$$\vec{K}_{3,n} = I_n \gamma_n \hat{z}; \quad (41)$$

$$\alpha_n = \frac{jM_n \sin \theta_i \cos \theta_i}{J_n(k_{\rho,r}a) R_n}; \quad (42)$$

$$\beta_n = \frac{nW \sin \theta_i \cos \theta_i}{J_n(k_{\rho,r}a) R_n}; \quad (43)$$

$$\gamma_n = \frac{jM_n \sin \theta_i}{J_n(k_{\rho,r}a) R_n}. \quad (44)$$

For a horizontally polarized excitation wave, the derivation for the scattering matrix elements $S_{ph}^l(\hat{k}_s, \hat{k}_i)$ closely follows the one outlined above; it is seen that they can be obtained from Eq. 38 simply by redefining α_n , β_n , and γ_n as

$$\alpha_n = \frac{-nW \sin \theta_i \cos^2 \theta_i}{J_n(k_{\rho,r}a)R_n}; \quad (45)$$

$$\beta_n = \frac{jN_n \sin \theta_i}{J_n(k_{\rho,r}a)R_n}; \quad (46)$$

$$\gamma_n = \frac{-nW \sin \theta_i \cos \theta_i}{J_n(k_{\rho,r}a)R_n}. \quad (47)$$

Expressions for $S_{pv}^l(\hat{k}_s, \hat{k}_i)$ and $S_{ph}^l(\hat{k}_s, \hat{k}_i)$ here match the formulations from Karam et al.¹⁷ (Note that there are typographical errors in Eq. 25 of that journal article.¹⁷)

3. Multiray Solution in the Presence of a Half Space

For the case when the cylinder is located above a finite-conducting ground (with the air-ground interface at $z = 0$), a total scattering matrix can be constructed by summing the direct wave from the cylinder and the ground-reflected waves. Succinctly, the first 4 main contributions can be written as

$$\begin{aligned} \bar{\bar{S}}(\hat{k}_s, \hat{k}_i) = & \bar{\bar{S}}^g(\hat{k}_s, \hat{k}_i) e^{-jk_o(\hat{k}_i \cdot \vec{r}_o - \hat{k}_s \cdot \vec{r}_o)} + \bar{\bar{S}}^g(\hat{k}_s, \hat{k}_{i,g}) \cdot \bar{\bar{\Gamma}}(\hat{k}_i) e^{-jk_o(\hat{k}_i \cdot \vec{r}_g - \hat{k}_s \cdot \vec{r}_o)} \\ & + \bar{\bar{\Gamma}}(\hat{k}_s) \cdot \bar{\bar{S}}^g(\hat{k}_{s,g}, \hat{k}_i) e^{-jk_o(\hat{k}_i \cdot \vec{r}_o - \hat{k}_s \cdot \vec{r}_g)} + \bar{\bar{\Gamma}}(\hat{k}_s) \cdot \bar{\bar{S}}^g(\hat{k}_{s,g}, \hat{k}_{i,g}) \cdot \bar{\bar{\Gamma}}(\hat{k}_i) e^{-jk_o(\hat{k}_i \cdot \vec{r}_g - \hat{k}_s \cdot \vec{r}_g)}, \end{aligned} \quad (48)$$

where \vec{r}_o is the location of the center of the cylinder; $\vec{r}_g = \vec{r}_o - 2(\vec{r}_o \cdot \hat{z})\hat{z}$; $\hat{k}_{i,g} = \hat{k}_i - 2(\hat{k}_i \cdot \hat{z})\hat{z}$; $\hat{k}_{s,g} = \hat{k}_s - 2(\hat{k}_s \cdot \hat{z})\hat{z}$; $\bar{\bar{S}}^g(\cdot, \cdot)$ is the cylinder response in free space; and $\bar{\bar{\Gamma}}(\hat{k}_{i,s})$ is the ground-reflection-coefficient matrix

$$\bar{\bar{\Gamma}}(\hat{k}_{i,s}) = \begin{bmatrix} r_v(\hat{k}_{i,s}) & 0 \\ 0 & r_h(\hat{k}_{i,s}) \end{bmatrix}, \quad (49)$$

with $r_v(\hat{k}_{i,s})$ and $r_h(\hat{k}_{i,s})$ as the ordinary horizontally and vertically polarized ground reflection coefficients, respectively. The first term in Eq. 48 is the direct wave from the cylinder; the second and third terms correspond to the single

ground bounce returns; and the last term is the double ground bounce contribution.

Note that if the global coordinate system is aligned with the local coordinate system used for the definition of $\overline{\overline{S}}^l(\cdot, \cdot)$ in Section 2, then $\overline{\overline{S}}^g(\cdot, \cdot) = \overline{\overline{S}}^l(\cdot, \cdot)$. Otherwise, for an arbitrarily oriented cylinder, the scattering matrix $\overline{\overline{S}}^g(\cdot, \cdot)$ should be modified as

$$\overline{\overline{S}}^g(\hat{k}_b, \hat{k}_a) = \begin{bmatrix} \hat{v}_s \cdot \hat{v}_s^{gl} & \hat{v}_s \cdot \hat{h}_s^{gl} \\ \hat{h}_s \cdot \hat{v}_s^{gl} & \hat{h}_s \cdot \hat{h}_s^{gl} \end{bmatrix} \cdot \overline{\overline{S}}^l(\hat{k}_b^l, \hat{k}_a^l) \cdot \begin{bmatrix} \hat{v}_i^{gl} \cdot \hat{v}_i & \hat{v}_i^{gl} \cdot \hat{h}_i \\ \hat{h}_i^{gl} \cdot \hat{v}_i & \hat{h}_i^{gl} \cdot \hat{h}_i \end{bmatrix}, \quad (50)$$

in which (\hat{v}_i, \hat{h}_i) , (\hat{v}_s, \hat{h}_s) , and (\hat{k}_a, \hat{k}_b) are the original global coordinate vectors; $(\hat{v}_i^{gl}, \hat{h}_i^{gl})$ and $(\hat{v}_s^{gl}, \hat{h}_s^{gl})$ are the polarization vectors in the cylinder's local coordinate system written in global coordinates—these correspond to \hat{k}_a^l and \hat{k}_b^l , respectively. Note that $\hat{k}_a^l = \overline{\overline{T}}^{lg} \hat{k}_a$ and $\hat{k}_b^l = \overline{\overline{T}}^{lg} \hat{k}_b$. Here, it is assumed that vector transformations from global to local coordinates (or vice versa) can be accomplished with a transformation matrix $\overline{\overline{T}}^{lg}$ (or $\overline{\overline{T}}^{gl} = \left(\overline{\overline{T}}^{lg}\right)^T$).

4. Numerical Results

The backscattering cross section of a tilted, finite-length, dielectric circular cylinder is shown in Figs. 1–3 for the free-space and half-space cases, as calculated with Eqs. 38 and 48. The cylinder has radius $a = 15$ cm and length $L = 7.5$ m and is centered at $\vec{r}_o \approx (0.49, 1.26, 3.58)$, with its axis parallel to the vector $(0.12, 0.32, 0.94)$. The cylinder and ground have relative dielectric constant and conductivity (ϵ_r, σ_d) of $(13.9, 39 \text{ mS/m})$ and $(5.45, 20 \text{ mS/m})$, respectively. The backscattering cross section is defined as $\sigma_{pq} = 4\pi \left| S_{pq}(-\hat{k}_i, \hat{k}_i) \right|^2$. The incidence angles here are set as $\theta_i = 40^\circ$ and $\phi_i = 200^\circ$. Because of the dihedral-like effect, an enhancement in the return is observed for the co-polarized responses when the cylinder is located above a ground; a similar effect is not apparent for the cross-polarized responses in this example. Note that reciprocity dictates $S_{hv} = -S_{vh}$ in the backscattering direction.¹⁸ Although the formulation given in Section 2 obeys this relation, the multiray approach given in Section 3

does not. In view of this deficiency in the half-space solution, the average cross-polarized response (that is, $(S_{hv} - S_{vh})/2$) is plotted in Fig. 3.

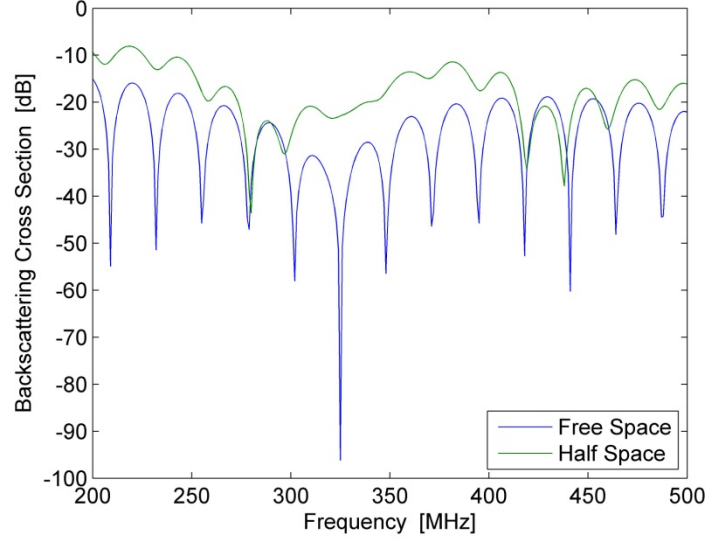


Fig. 1 Backscattering cross section (as function of frequency) of a tilted, finite-length, dielectric circular cylinder located in free space and above a half space: vv response. Parameters: $a = 15$ cm; $L = 7.5$ m; $\theta_i = 40^\circ$; and $\phi_i = 200^\circ$.

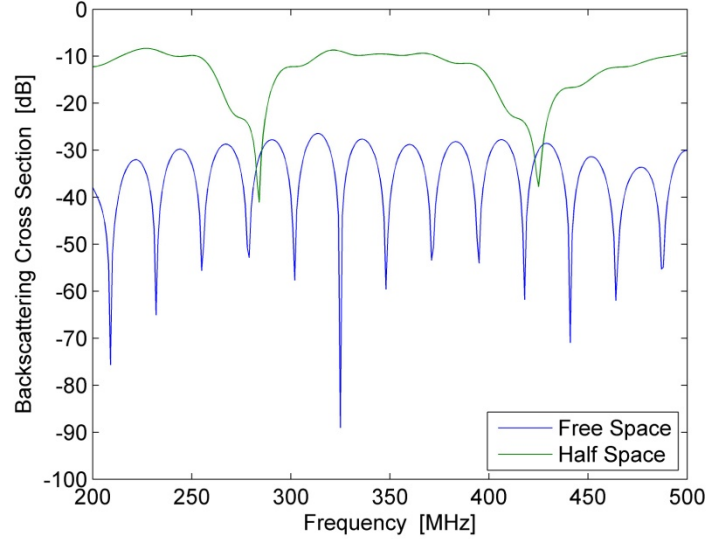


Fig. 2 Backscattering cross section (as function of frequency) of a tilted, finite-length, dielectric circular cylinder located in free space and above a half space: hh response. Parameters are the same as those in Fig. 1.

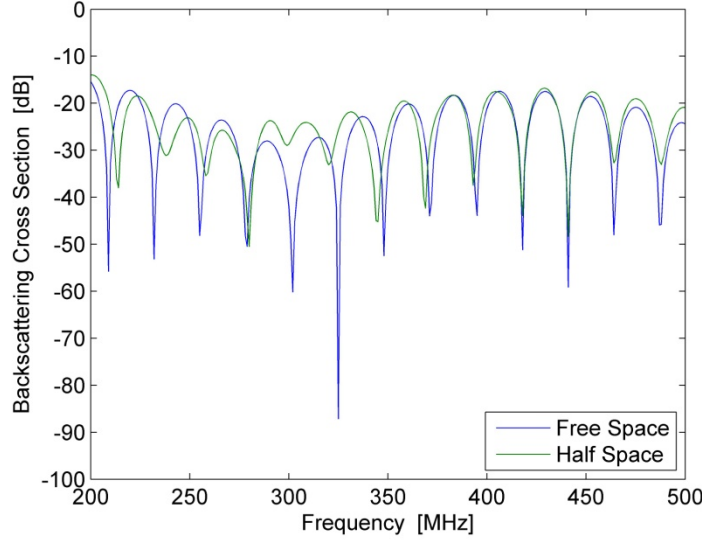


Fig. 3 Backscattering cross section (as function of frequency) of a tilted, finite-length, dielectric circular cylinder located in free space and above a half space: $h\nu$ response. Parameters are the same as those in Fig. 1.

5. Conclusions

The complete derivation of a closed-form formulation for the scattering matrix of the finite-length, dielectric circular cylinder has been presented. The semi-exact solution is obtained by approximating the internal fields of the finite-length cylinder with those of the infinite-length case, which has an exact solution available through modal analysis. Application of the volumetric equivalence principle enables the generalized far-field response of the scatterer to be characterized in an efficient manner. The theory is first developed for a cylinder in free space; subsequently, the problem of the cylinder located above a flat dielectric ground is considered with a multiray technique in which the ground effects are taken into account through the introduction of reflection coefficient matrices and phase delay terms. The scattering response of an arbitrarily oriented cylinder is obtained by supplementing the canonical formulation with appropriate coordinate transformation matrices. The complete solution established above facilitates the development of the discrete scatterer approach for characterizing the scattering return from tree structures. An evaluation of the accuracy of the solution and a determination of its region of validity is the subject of Part II of this study.

6. References

1. Lang RH, Sidhu JS. Electromagnetic backscattering from a layer of vegetation: a discrete approach. *IEEE Trans Geosci Rem Sens.* 1983;21(1):62–71.
2. Richards JA, Sun G-Q, Simonett DS. L-band radar backscatter modeling of forest stands. *IEEE Trans Geosci Rem Sens.* 1987;25(4):487–498.
3. Ulaby FT, Sarabandi K, McDonald K, Whitt M, Dobson MC. Michigan microwave canopy scattering model (MIMICS). Ann Arbor (MI): University of Michigan Radiation Laboratory; 1988. Report No.: 022486-T-1.
4. Durden SL, van Zyl JJ, Zebker HA. Modeling and observation of the radar polarization signature of forested areas. *IEEE Trans Geosci Rem Sens.* 1989;27(3):290–301.
5. McDonald KC, Dobson MC, Ulaby FT. Using MIMICS to model L-band multiangle and multitemporal backscatter from a walnut orchard. *IEEE Trans Geosci Rem Sens.* 1990;28(4):477–491.
6. Ulaby FT, Sarabandi K, McDonald K, Whitt M, Dobson MC. Michigan microwave canopy scattering model. *Int J Rem Sens.* 1990;11:1223–1253.
7. Chauhan NS, Lang RH, Ranson KJ. Radar modeling of a boreal forest. *IEEE Trans Geosci Rem Sens.* 1991;29(4):627–638.
8. Yueh SH, Kong JA, Jao JK, Shin RT, Toan TL. Branching model for vegetation. *IEEE Trans Geosci Rem Sens.* 1992;30(2):390–402.
9. Hsu C-C, Kong JA, Toups MF, Fleischman JG, Ayasli S, Shin RT. Electromagnetic modeling of foliage-obscured point source response. *Proceedings of SPIE 1942, Underground and Obscured Object Imaging and Detection*; 1993 Apr 11; Orlando, FL.
10. Lin Y-C, Sarabandi K. Electromagnetic scattering model for a tree trunk above a tilted ground plane. *IEEE Trans Geosci Rem Sens.* 1995;33(4):1063–1070.
11. Lin Y.-C. A fractal-based coherent scattering and propagation model for forest canopies [dissertation]. [Ann Arbor (MI)]: University of Michigan; 1997.
12. Tsang L, Kong JA, Ding K-H, Ao CO. Scattering of electromagnetic waves: numerical simulations. 1st ed. New York (NY): John Wiley and Sons; 2001.

13. Picard G, Le Toan T, Quegan S, Caraglio Y, Castel T. Radiative transfer modeling of cross-polarized backscatter from a pine forest using the discrete ordinate and eigenvalue method. *IEEE Trans Geosci Rem Sens.* 2004;42(8):1720–1730.
14. Thirion L, Colin E. On the use of a coherent scattering model to determine the origin of artificial signatures of a target hidden in a forest. In: Lacoste H, editor. *POLINSAR 2005. Proceedings of the 2nd International Workshop*; 2005 Jan 17–21; Frascati, Italy: European Space Agency.
15. Liang P, Pierce LE, Moghaddam M. Radiative transfer model for microwave bistatic scattering from forest canopies. *IEEE Trans Geosci Rem Sens.* 2005;43(11):2470–2483.
16. Liang P, Moghaddam M, Pierce LE, Lucas RM. Radar backscattering model for multilayer mixed-species forests. *IEEE Trans Geosci Rem Sens.* 2005;43(11):2612–2626.
17. Karam MA, Fung AK, Antar YMM. Electromagnetic wave scattering from some vegetation samples. *IEEE Trans Geosci Rem Sens.* 1988;26(6):799–808.
18. Ulaby FT, Elachi C, editors. *Radar polarimetry for geoscience applications.* Norwood (MA): Artech House; 1990.

1 DEFENSE TECHNICAL
(PDF) INFORMATION CTR
DTIC OCA

2 DIRECTOR
(PDF) US ARMY RESEARCH LAB
RDRL CIO LL
IMAL HRA MAIL & RECORDS MGMT

1 GOVT PRINTG OFC
(PDF) A MALHOTRA

1 DIRECTOR
(PDF) US ARMY RESEARCH LAB
RDRL SER

4 DIRECTOR
(PDF) US ARMY RESEARCH LAB
RDRL SER U
D LIAO
T DOGARU
A SULLIVAN